Journal of Visualized Experiments

Use of the Patch-clamp Technique to Study the Thermogenic Capacity of Mitochondria

--Manuscript Draft--

Article Type:	Invited Methods Collection - JoVE Produced Video
Manuscript Number:	JoVE62618R2
Full Title:	Use of the Patch-clamp Technique to Study the Thermogenic Capacity of Mitochondria
Corresponding Author:	Ambre Bertholet UCLA Medical School: University of California Los Angeles David Geffen School of Medicine Los Angeles, CA UNITED STATES
Corresponding Author's Institution:	UCLA Medical School: University of California Los Angeles David Geffen School of Medicine
Corresponding Author E-Mail:	abertholet@mednet.ucla.edu
Order of Authors:	Ambre Bertholet
Additional Information:	
Question	**Response**
Please specify the section of the submitted manuscript.	Biology
Please indicate whether this article will be Standard Access or Open Access.	Standard Access ($1400)
Please indicate the **city, state/province, and country** where this article will be **filmed**. Please do not use abbreviations.	Los Angeles, California, USA
Please confirm that you have read and agree to the terms and conditions of the author license agreement that applies below:	I agree to the Author License Agreement
Please provide any comments to the journal here.	

TITLE:

The Use of the Patch-Clamp Technique to Study the Thermogenic Capacity of Mitochondria

AUTHORS AND AFFILIATIONS:

Ambre M. Bertholet[1]

[1]Department of Physiology, David Geffen School of Medicine, University of California Los Angeles

Email Address of the Author:

Ambre M. Bertholet (abertholet@mednet.ucla.edu)

SUMMARY:

This method article details the main steps in measuring H^+ leak across the inner mitochondrial membrane with the patch-clamp technique, a new approach to study the thermogenic capacity of mitochondria.

ABSTRACT:

Mitochondrial thermogenesis (also known as mitochondrial uncoupling) is one of the most promising targets for increasing energy expenditure to combat metabolic syndrome. Thermogenic tissues such as brown and beige fats develop highly specialized mitochondria for heat production. Mitochondria of other tissues, which primarily produce ATP, also convert up to 25% of the total mitochondrial energy production into heat and can, therefore, have a considerable impact on the physiology of the whole body. Mitochondrial thermogenesis is not only essential for maintaining the body temperature, but also prevents diet-induced obesity and reduces the production of reactive oxygen species (ROS) to protect cells from oxidative damage. Since mitochondrial thermogenesis is a key regulator of cellular metabolism, a mechanistic understanding of this fundamental process will help in the development of therapeutic strategies to combat many pathologies associated with mitochondrial dysfunction. Importantly, the precise molecular mechanisms that control acute activation of thermogenesis in mitochondria are poorly defined. This lack of information is largely due to a dearth of methods for the direct measurement of uncoupling proteins. The recent development of patch-clamp methodology applied to mitochondria enabled, for the first time, the direct study of the phenomenon at the origin of mitochondrial thermogenesis, H^+ leak through the IMM, and the first biophysical characterization of mitochondrial transporters responsible for it, the uncoupling protein 1 (UCP1), specific of brown and beige fats, and the ADP/ATP transporter (AAC) for all other tissues. This unique approach will provide new insights into the mechanisms that control H^+ leak and mitochondrial thermogenesis and how they can be targeted to combat metabolic syndrome. This paper describes the patch-clamp methodology applied to mitochondria to study their thermogenic capacity by directly measuring H^+ currents through the IMM.

INTRODUCTION:

Mitochondria are famous for being the powerhouse of the cell. Indeed, they are the major source of chemical energy, ATP. What is less known is that mitochondria also generate heat. In fact, every mitochondrion constantly generates the two types of energies (ATP and heat) and a fine

balance between the two energy forms defines metabolic cell homeostasis (**Figure 1**). How mitochondria distribute energy between ATP and heat is certainly the most fundamental question in the field of bioenergetics, although it is still largely unknown. We do know that increasing mitochondrial heat production (called mitochondrial thermogenesis), and consequently reducing ATP production increases energy expenditure and this is one of the best ways to combat metabolic syndrome[1].

Mitochondrial thermogenesis originates from H^+ leak across the inner mitochondrial membrane (IMM), leading to uncoupling of substrate oxidation and ATP synthesis with consequent production of heat, hence the name "mitochondrial uncoupling"[1] (**Figure 1**). This H^+ leak depends on mitochondrial transporters called uncoupling proteins (UCPs). UCP1 was the first UCP identified. It is only expressed in thermogenic tissues, brown fat, and beige fat in which mitochondria are specialized for heat production[2–4]. The identity of UCP in non-adipose tissues such as skeletal muscle, heart, and liver, has remained controversial. Mitochondria in these tissues can have about 25% of the total mitochondrial energy converted into heat, which can significantly impact the physiology of the whole body[1]. Besides maintaining core body temperature, mitochondrial thermogenesis also prevents diet-induced obesity by reducing calories. In addition, it reduces the production of reactive oxygen species (ROS) by mitochondria to protect cells from oxidative damage[1]. Thus, mitochondrial thermogenesis is involved in normal aging, age-related degenerative disorders, and other conditions involving oxidative stress, such as ischemia-reperfusion. Therefore, mitochondrial thermogenesis is a powerful regulator of cellular metabolism, and a mechanistic understanding of this fundamental process will promote the development of therapeutic strategies to combat many pathologies associated with mitochondrial dysfunction.

Mitochondrial respiration was the first technique to reveal the crucial role of mitochondrial thermogenesis in cellular metabolism and is still the most popular in the community[1]. This technique is based on the measurement of oxygen consumption by the mitochondrial electron transport chain (ETC) that increases when mitochondrial H^+ leak is activated. This technique, although instrumental, cannot directly study mitochondrial H^+ leak across the IMM[1], thereby making the precise identification and characterization of the proteins responsible for it difficult, particularly in non-adipose tissues in which heat production is secondary as compared to ATP production. Recently, the development of the patch-clamp technique applied to mitochondria, provided the first direct study of H^+ leak across the whole IMM in various tissues[5–7].

The mitochondrial patch-clamp of the whole IMM was first established in a reproducible way by Kirichok et al.[8]. They described the first direct measurement of mitochondrial calcium uniporter (MCU) currents in 2004 using mitoplasts from COS-7 cell lines[8]. Later, the Kirichok lab showed calcium currents from IMMs of mouse[9] and *Drosophila* tissues[9]. Other labs now routinely use this technique to study the biophysical properties of MCU[10–14]. Whole IMM patch-clamp analysis of potassium and chloride conductance is also possible and has been mentioned in several papers but has not yet been published[6,7,9]. The first measurement of H^+ currents across the IMM was reported in 2012 from mouse brown fat mitochondria[6], and from mouse beige fat mitochondria in 2017[7]. This current is due to the specific uncoupling protein of thermogenic tissues, UCP1[6,7].

Recent work published in 2019 characterized AAC as the main protein responsible for mitochondrial H^+ leak in non-adipose tissues such as the heart and skeletal muscle[5].

This unique approach now allows for the direct high-resolution functional analysis of the mitochondrial ion channels and transporters responsible for mitochondrial thermogenesis. To facilitate the expansion of the method and to complement other studies such as mitochondrial respiration, a detailed protocol is described below for measuring the H^+ currents carried by UCP1 and AAC. Three important steps are described: 1) mitochondrial isolation from mouse brown fat to analyze UCP1-dependent H^+ current and mitochondrial isolation from the heart to analyze AAC-dependent H^+ current, 2) preparation of mitoplasts with a French Press for mechanical rupture of the outer mitochondrial membrane (OMM), 3) patch-clamp recordings of UCP1 and AAC-dependent H^+ currents across the whole IMM.

PROTOCOL:

All animal experimental procedures that were performed conform to the National Institutes of Health guidelines and were approved by the University of California Los Angeles Institutional Animal Care and Use Committee (IACUC).

NOTE: The mitochondrial isolation procedure is based on differential centrifugation and varies slightly from tissue to tissue. For example, since brown adipose tissue is extremely rich in lipids, it requires an additional step to separate cell debris and organelles from the lipid phase before harvesting the mitochondria. To avoid confusion, the two mitochondrial isolation procedures (one from the brown fat and the other from the heart) are detailed below.

1. Mitochondrial isolation from mouse interscapular brown fat (modified from Bertholet et al. 2020)[15]

1.1. Euthanize C57BL/6 male mouse using CO_2 asphyxiation and subsequent cervical dislocation, as recommended by the American Veterinary Medical Association Panel and the IACUC Committee.

1.2. After positioning the mouse with its belly facing the table, spray alcohol to clean and wet the hair (modified from Mann et al., 2014)[16].

1.3. Make an incision of 2 cm in the upper back after grasping the skin with tweezers.

1.4. Extract the brown interscapular fat of the mouse that corresponds to a two-lobed organ with a butterfly shape[16].

1.5. Transfer the brown fat to a 35 mm Petri dish filled with 5 mL of cold isolation buffer previously placed on ice.

1.6. Clean the brown fat from the white fat under a binocular.

1.7. Transfer the brown fat to a 10 mL beaker with 5 mL of cold isolation buffer (**Table 1**) to chop it up into thin pieces. Transfer to the ice-chilled 10 mL glass homogenizer (plastic material polytetrafluoroethylene (PTFE) pestle).

1.8. Use an overhead stirrer to homogenize the pre-cut tissue on ice with six gentle strokes at a controlled speed of 275 rotations/min.

1.9. Centrifuge the homogenate at 8,500 x *g* for 10 min at 4 ˚C in a 15 mL ice-cold conical tube. Discard the supernatant containing the lipid phase.

1.6. Resuspend the pellet in 5 mL of ice-cold isolation buffer (**Table 1**) and homogenize, a second time, the suspension on ice with six slow strokes at a speed of 275 rotation/min.

1.7. Transfer the homogenate in a 15 mL ice-cold conical tube and centrifuge it at 700 x *g* for 10 min at 4 ˚C To pellet all nuclei and unbroken cells.

1.8. Collect the supernatant in a fresh 15 mL tube and place it on ice.

1.9. Centrifuge the supernatant at 8,500 x *g* for 10 min at 4 ˚C to obtain a pellet containing mitochondria.

1.10. Resuspend pellet containing mitochondria in 3.8 mL of ice-cold hypertonic-mannitol buffer (**Table 2**) and incubate the mitochondrial suspension on ice for 10–15 min.

2. Mitochondrial isolation from the mouse heart (modified from Garg et al. 2019)[17]

2.1. Euthanize C57BL/6 male mouse using CO_2 asphyxiation and subsequent cervical dislocation, as recommended by the American Veterinary Medical Association Panel and the IACUC Committee.

2.2. After positioning the mouse on its back, spray alcohol to clean and wet the hair. Then, make a 2 cm incision on the thorax after grasping the skin with tweezers.

2.3. Dissect the heart from the animal's chest and rinse it to remove all the blood in a 10 mL beaker with 5 mL of the cold isolation solution.

2.4. Once the heart has been cleared of traces of blood, transfer it to another 10 mL beaker containing 5 mL of cold isolation buffer (**Table 1**) to chop it up into thin pieces. Then, transfer to an ice-chilled 10 mL glass homogenizer (PTFE pestle).

2.5. Use an overhead stirrer to homogenize the pre-cut tissue on ice with six gentle strokes at a controlled speed of 275 rotations/min.

2.6. Transfer the homogenate to a 15 mL ice-cold conical tube and centrifuge it at 700 x *g* for 10

min at 4 ˚C to pellet nuclei and unbroken cells.

2.7. Collect the supernatant in a fresh 15 mL tube and place it on ice.

2.8. Centrifuge the supernatant at 8,500 x *g* for 10 min at 4 ˚C to obtain a pellet containing mitochondria.

2.9. Resuspend the mitochondrial pellet in 3.8 mL of ice-cold hypertonic-mannitol buffer (**Table 2**) and incubate the mitochondrial suspension on ice for 10–15 min.

3. Preparation of mitoplasts with a French Press for mechanical rupture of the OMM.

NOTE: The French press procedure allows the IMM to be released from the OMM with its integrity preserved, including the matrix and crista (**Figure 2**)[18]. Mitochondria are pre-incubated in a hypertonic-mannitol buffer (**Table 2**) and subjected to a lower pressure during the French press procedure to avoid any drastic stretching of the IMM when the OMM is ruptured.

3.1. Fill the mitochondrial-hypertonic-mannitol suspension into a refrigerated mini pressure cell (piston diameter 3/8") of the French press (**Figure 3A**).

3.2. Select the **Medium** mode of the French Press and compress the suspension through the mini pressure cell at 110 on the dial of the French Press for the brown fat mitochondria and at 140 for the heart mitochondria. Ensure that the suspension comes out of the mini pressure cell at a rate of about 1 drop/s.

3.3. Collect the drops in a 15 mL ice-chilled conical tube.

3.4. Centrifuge the suspension at 10,500 x *g* for 10 min at 4 ˚C.

3.5. Resuspend the mitoplasts pellet in 0.5–2 mL of ice-cold Hypertonic-KCl buffer (**Table 3**) and store the suspension on ice.

NOTE: Brown fat and heart mitoplasts are ready for patch-clamp recordings and should remain usable for about 3–6 h.

4. Electrophysiological recordings of H^+ leak through UCP1 and AAC[5,7,15]

NOTE: Use the following electrophysiological setup (**Figure 3B**): inverted microscope with differential interference contrast (DIC), 60x water immersion objective, vibration isolation table and a Faraday cage, a standard amplifier supporting low-noise recordings, a standard digitizer used for electrophysiological setup, pClamp 10, a micromanipulator, bath reference electrode (3 M KCl-agar salt bridge inserted within a microelectrode holder containing a silver/silver chloride pellet molded into the holder body (described in Liu et al. 2021)[19], perfusion chamber with a 0.13 mm glass coverslip bottom, connected to a gravity-fed perfusion system.

4.1. Pull the borosilicate glass filaments on the day of recording using a micropipette puller. Set a program on the puller used for generating pipettes with a high degree of reproducibility[20].

NOTE: This program design requires several tries to obtain pipettes optimized for the IMM patch-clamp. A standard pipette has fine tips with a progressive conic shape.

4.2. Insert one glass filament within the puller and pull to obtain almost two identical patch pipettes from one borosilicate filament.

4.3. Adjust the program when pipettes become inconsistent between pulling cycles due to aging of the heating box filament of the puller.

4.4. Position the pipette inside the pipette polisher and place the tip near the filament under 100x magnification to fire-polish it.

4.5. Press the foot pedal several times to heat the filament without clogging or damaging the tip curve.

4.6. Polish until pipettes with a resistance between 25 and 35 MΩ are obtained when filled with TMA-based pipette solution (TMA for tetramethylammonium hydroxide, **Table 4**).

4.7. Pre-incubate coverslips (5 mm diameter, 0.1 mm thickness) with 0.1% gelatin to reduce the mitoplast adhesion and rinse them with the KCl bath solution (**Table 5**) before depositing the mitoplast suspension.

4.8. Prepare a raw dilution by mixing ~35 µL of the concentrated mitoplast suspension with 500 µL of the KCl bath solution (**Table 5**) and place it on coverslips previously placed in a well of a 4-well plate.

4.9. Incubate on ice for 15 to 20 min for mitoplasts to sediment on the coverslip.

4.10. Fill the bath chamber completely with ~50 µL of the KCl bath solution (**Table 5**).

4.11. Transfer a coverslip with mitoplasts within the chamber using thin microdissection tweezers with a bent tip.

4.12. Arrange the coverslip at the bottom of the chamber. Do not perfuse the chamber to keep the mitoplasts stable on the coverslip.

4.13. Choose an individual non-adhesive mitoplast in the shape of 8 by scanning the coverslip under the microscope with a 60x objective.

4.14. Load the pipette with the pipette solution (~50 µL) and place it in the pipette holder.

4.15. Bring the pipette into the bath solution with a micromanipulator and approach it just above the selected mitoplast to get close to the IMM. The amplifier program gives the resistance of the pipette once it is in the bath solution. Hold the membrane potential at 0 mV and apply 10 mV pulses using the membrane test command in the amplifier program.

4.16. Apply slight negative pressure to quickly create a gigaseal with the IMM (**Figure 2B**).

4.17. Rise the pipette with the mitoplast attached to keep them away from the coverslip to avoid the seal breakage due to the pipette drift during the experiment.

4.18. Compensate the stray capacitance transients with the "membrane test" command in the amplifier program before testing the whole-mitoplast configuration to obtain a correct capacitance (Cm) measurement for the mitoplast membrane after the break-in.

4.19. Apply short-duration (5–15 ms) voltage pulses (250–600 mV) with the amplifier program to rupture the membrane patch under the glass pipette and achieve the whole-mitoplast configuration (**Figure 2C**). Successful break-in is reflected by the reappearance of capacitance transients.

4.20. After the break-in, fit the capacitance transients with the amplifier program's membrane test option to assess the membrane capacitance (reflecting the size of the mitoplast) and its access resistance Ra (reflecting the quality of the whole-mitoplast configuration). After the break-in, Ra should be between 40 and 80 MΩ. Mitoplasts (2–6 µm in size) used for patch-clamp experiments typically have membrane capacitances of 0.5–1.1 pF.

4.21. Immediately after the break-in, replace the KCl bath solution (**Table 5**) with the HEPES bath solution (**Table 6**) by starting the perfusion.

4.22. Apply an 850 ms ramp protocol designed with the amplifier program, from -160 mV to +100 mV with a 5 s interval, while holding the mitoplast at 0 mV. This protocol works for UCP1[6,7,15] and AAC[5] studies (**Figure 4** and **Figure 5**).

NOTE: It is recommended for UCP1 and AAC-dependent H^+ current measurements to acquire all electrophysiological data at 10 kHz and to filter at 1 kHz using adequate software driving the amplifier and digitizer.

REPRESENTATIVE RESULTS:

The development of the patch-clamp methodology applied to mitochondria provided the first direct study of H^+ leak through the IMM and the mitochondrial transporters, UCP1 and AAC, which are responsible for it. The electrophysiological analysis of UCP1- and AAC-dependent H^+ leaks can provide a first glance of the thermogenic capacity of mitochondria. The results section describes the standard procedures to measure H^+ leak via UCP1 and AAC.

UCP1-dependent H^+ current measurement (Figure 4)[6,7,15]

Application of the voltage ramp protocol induces a large-amplitude H^+ current across the IMM of brown fat without the addition of exogenous fatty acids (FA), the required activators of UCPs (**Figure 4A**). This is a specific characteristic of brown and beige fat IMM due to the local production of FA by a phospholipase activity associated with the membrane. When the H^+ current develops in response to the ramp protocol, it is important to wait for the current amplitude to stabilize. Quantification of the H^+ current amplitude via UCP1 requires the determination of the baseline corresponding to a zero UCP1 current. Once the stability of the H^+ current amplitude is reached, it is recommended to perfuse either UCP1 inhibitor Guanosine diphosphate (GDP - 1 mM, **Figure 4A**) or a FA chelator (0.5% FA-free bovine serum albumin, not shown) or 10 mM Methyl Beta Cyclodextrin (MβCD) for the endogenous membrane FA extraction, **Figure 4B**, black trace). The residual current is the current from which the amplitude of the UCP1 currents will be determined. To help compare the amplitudes of UCP1 currents in different mitoplasts, the current density (pA/pF) of each mitoplast is calculated by normalizing the UCP1 currents with the mitoplast capacitance (Cm)[5,7]. The current can be reactivated by the addition of exogenous long chain FA using arachidonic acid (AA) or oleic acid (OA) (1–2 µM). Since both brown and beige fat IMMs possess PLA2 activity, endogenous membrane FAs are partially regenerated within a few minutes of washing the MβCD/albumin from the bath, leading to reactivation of the H^+ current via UCP1[6,7]. As expected, this current disappears completely in the IMM of *UCP1*$^{-/-}$ mice (**Figure 4A**)[6,7].

A more precise way to compare the density and activity of UCP1 of different mitoplasts of the same tissue or of mitoplasts from different tissues (brown and beige fat) is to control FA concentration at the surface of the IMM[6,7]. Indeed, H^+ current amplitude could vary between mitoplasts due to the UCP1 protein amount per IMM but also due to the production of endogenous FA. Thus, it is recommended to extract endogenous FA from the IMM and to reactivate UCP1-dependent H^+ current by adding exogenous FA at a known concentration. To do this, endogenous FAs must first be extracted from the IMM by perfusing a HEPES bath solution (**Table 6**) containing 10 mM MβCD. Then, to allow the reactivation of the H^+ current via UCP1 by only a precise concentration of exogenous FAs, the latter will be perfused on a HEPES/MβCD background to continuously extract FAs produced from the IMM.

The study of the competition between the purine nucleotide and FA for binding to UCP1 is also possible with the patch-clamp technique[6,7,15]. Inhibition of UCP1 by purine nucleotides (e.g., Mg^{2+}-free ATP) can be compared to two different concentrations of FA (ideally 10-fold). For this purpose, endogenous membrane FA are first removed by applying 10 mM MβCD (**Figure 4B**, black trace). Application of exogenous FAs (e.g., here, only 0.5 mM FAs are shown) applied on a background of 10 mM MβCD allows precise control of the concentration of activating FAs because locally produced FAs are immediately extracted from the membrane. In this condition, exogenous FAs are primarily responsible for the development of the H^+ current. Different concentrations of ATP are subsequently added to the OA/MβCD solution to assess the $IC50_{ATP}$ for each FA concentration tested and thus, establish whether FA compete with purine nucleotides for binding to UCP1.

AAC-dependent H^+ current measurement (Figure 5)[5]

Unlike brown fat, the IMM of non-adipose tissues such as skeletal muscle and the heart does not develop a measurable H^+ immediately after the break-in (**Figure 5**, black traces). To induce a measurable H^+ current through AAC, it is essential to apply the HEPES bath solution (**Table 6**) containing 1–2 µM of exogenous FA (AA, **Figure 5A**, red trace). This may indicate that the IMM of non-adipose tissues does not have a FA production machinery into the IMM as is found in the IMM of brown and beige fats.

The baseline (or zero current) for the quantification of the H^+ current amplitude via AAC corresponds to the HEPES bath solution (**Table 6**) perfused on the surface of the IMM prior to the addition of FA. To confirm that the measured H^+ current is carried by AAC, it is important to apply specific inhibitors of AAC added to FA, 1 µM of carboxyatractyloside (CATR, **Figure 5A**) or 4 µM of bonkgrekic acid (BKA, not shown)[5], which almost completely inhibit H^+ current. This current disappears completely in the IMM of *AAC1*$^{-/-}$ mice (**Figure 5A**), AAC1 being the predominant isoform in the heart[5].

Patch-clamp analysis of the interaction between FA-dependent H^+ leak and nucleotides is also possible with AAC[5]. However, there is an important difference between AAC and UCP1: AAC not only carries H^+ but its main function is to transport adenine nucleotides ADP and ATP[21]. To study how adenine nucleotide exchange affects FA-dependent H^+ leak, 1 mM Mg^{2+}-free ADP is added to the pipette solution. Then, FA are perfused to activate H^+ current via AAC. Only ADP in the pipette solution does not interfere with the H^+ current[5]. Once a stable H^+ current amplitude is reached, ADP is perfused simultaneously with FA. Only when ADP is present on both sides of the membrane to generate an active nucleotide exchange via AAC is a constant but never complete inhibition of H^+ leak achieved (**Figure 5B**). This may indicate that the two transport modes of AAC (FA-H^+ current and ADP/ATP exchange) compete and are likely to occur via the same translocation pathway. The ADP/ADP homoexchange was selected to avoid the additional current associated with the physiological ADP/ATP heteroexchange[5].

FIGURE AND TABLE LEGENDS:

Figure 1: Mitochondrial energy distribution between heat and ATP production. Mechanisms of mitochondrial ATP and heat production. Mitochondria have two membranes [the OMM (purple) and the IMM (orange)], which contain the machinery for ATP and heat production. The ETC generates an electrochemical gradient of H^+ across the IMM, which is used by ATP synthase (AS) to produce ATP and used by UCPs to generate heat.

Figure 2: Mitochondrial patch-clamp technique (modified from Bertholet et al. 2020)[15]. (**A**) Mitochondria are isolated from tissue lysate by centrifugation (OMM in purple and IMM in orange). (**B**) Low-pressure French press ruptures the OMM to release the IMM which gives a mitoplast. Left panel represents a mitoplast, which assumes an 8-shaped form with remnants of the OMM attached to the IMM. A glass pipette is approached to the IMM to form a gigaohm seal (mitoplast-attached configuration). A photograph of the mitoplast-attached configuration is shown in the right panel. (**C**) The configuration of the whole-IMM (diagram in the left panel) is

obtained after breaking the membrane patch under the pipette by several voltage pulses (200–500 mV). A photograph of the whole IMM configuration is shown in the right panel. Inward currents (*I*, red) are negative.

Figure 3: French Press and electrophysiological setup. (**A**) Picture of French Press, which helps rupture the OMM to release the IMM. (**B**) Picture of a Faraday cage, inverted microscope with differential interference contrast (DIC), 60x water immersion objective, a vibration isolation table, and a micromanipulator. The standard amplifier, a standard digitizer, and PC computer are not shown in the picture.

Figure 4: H^+ current via UCP1 in brown fat. (**A**) Representative UCP1-dependent H^+ current recorded from brown fat mitoplast isolated from WT (upper panel) and *UCP1*$^{-/-}$ mice (lower panel). The control H^+ current traces shown in black correspond to the stabilized current amplitude after the IMM has been broken. 1 mM GDP is then added to the bath solution (orange). The voltage ramp protocol is shown above the WT traces. The pH of the bath and pipette solutions are shown in the pipette-mitoplast diagram. (**B**) Inhibition of UCP1 by purine nucleotides in brown fat. Representative UCP1-dependent H^+ current traces in various concentrations of ATP on the cytosolic face of the IMM of brown fat of mice at thermoneutrality. UCP1-dependent H^+ current was activated with 0.5 mM oleic acid (OA) mixed with 10 mM MβCD. The voltage protocol is indicated at the top. In the lower panel, the same trace is represented but not normalized with the mitoplast membrane capacitance. The brown fat mitoplast in this figure had a membrane capacitance of 0.624 pF.

Figure 5: FA-dependent H^+ current via AAC in heart mitoplast. (**A**) Representative AAC-dependent H^+ current when applied 2 µM AA in the bath solution (upper panel, orange) in WT heart mitoplasts and inhibited by 1 µM CATR (purple). Representative trace recorded in *AAC1*$^{-/-}$ heart mitoplast are in lower panel. Control current is in black. The voltage ramp protocol is shown above the WT traces. The pH of the bath and pipette solutions are shown in the pipette-mitoplast diagram. (**B**) While pipette solution contained 1 mM ADP, AAC-dependent H^+ current is induced by 2 µM AA (orange) and inhibited by addition of 1 mM ADP to bath (purple). The voltage ramp protocol is shown above the trace. The pH of the bath and pipette solutions are shown in the pipette-mitoplast diagram.

Table 1: Mitochondrial isolation buffer (tonicity ~ 300 mmol per kg)

Table 2: Hypertonic-mannitol buffer

Table 3: Hypertonic-KCl buffer

Table 4: TMA-based pipette solution (tonicity ~ 360 mmol per kg)

Table 5: KCl bath solution (tonicity ~ 300 mmol per kg)

Table 6: HEPES bath solution (tonicity ~ 300 mmol per kg)

DISCUSSION:

This method article aims to present the patch-clamp technique recently applied to mitochondria, a new approach to directly study H^+ leak through the IMM responsible for mitochondrial thermogenesis[5–7,15]. This technique is not limited to tissues and can also be used to analyze H^+ leak and other conductances of the IMM in different standard human and cell models such as HAP1, COS7, C2C12, and MEF cells. However, each mitochondrial isolation requires some readjustments specific to each cell or tissue type.

The main steps in the direct measurement of H^+ currents through the IMM of brown fat[5,6] and the heart[5] are summarized here to illustrate the mechanisms responsible for mitochondrial thermogenesis in specialized thermogenic and non-adipose tissues. Indeed, the development of this technique for the first time allows high-resolution functional analysis of the two main UCPs (UCP1 and AAC) in their native membrane environment with precise control of critical experimental conditions such as: 1) pH of pipette and bath solutions, 2) control of membrane potential across the IMM, and 3) precise composition of solutions to exclude any ions and metabolites permeable to the IMM other than H^+. The TMA-based pipette (**Table 4**) and HEPES bath solutions (**Table 6**) are formulated to record H^+ currents and contain only salts that dissociate into large anions and cations normally impermeable to the IMM. While the bath solution can be changed using a perfusion system, allowing different treatments to be applied to the cytosolic side of the membrane, it is not possible to change the composition of the intrapipette solution. This limits the understanding of the regulatory mechanisms that occur on the matrix side. Indeed, compounds must be present within the intrapipette solution at the time of filling the pipette. Therefore, H^+ leak can be studied in isolation of other currents. Pharmacological studies and the use of KO mice were essential for the characterization and identification of the proteins responsible for the H^+ current through the IMM of various tissues[5–7]. These results established that UCP1 is the main UCP of brown and beige fat, and AAC in non-adipose tissues. We cannot completely exclude the possibility of the existence of other H^+ currents not mediated by UCP1 and AAC. However, if other H^+ currents exist, their amplitude was beyond the resolution of our electrophysiological setup. We do not measure H^+ pumping of the ETC under the conditions described in this paper. Once we have reached the full IMM configuration, the mitochondrial matrix is washed out by perfusion of the intra-pipette solution. The intermembrane space no longer exists since the step of breaking the OMM with the French Press. No substrates of the respiratory complexes crucial for H^+ pumping through the ETC have been added. It is therefore unlikely to develop active H^+ pumping under the electrophysiological conditions detailed here.

Single channel recordings of excised patches are not described in this article. Although UCP1- and AAC-dependent H^+ currents across the IMM are robust due to their high protein density, the single-channel openings could not be resolved because the amplitude of UCP1 and AAC unitary currents are probably too small.

In contrast to biochemical studies, the mitochondrial isolation described in this article does not need to result in a high level of mitochondrial purity. Indeed, the mitochondrial preparation

consisting of a multitude of individualized mitoplasts and cell debris is scanned under the microscope to find one 8-shaped mitoplast to patch. The 8-shaped form of the mitoplast is due to release of the IMM through a hole in the OMM caused by the French press procedure (**Figure 2**). The less dense lobe corresponds to the IMM[15,17]. A suitable preparation can be defined by freely moving mitoplasts that can be easily distinguished from cellular debris. It is, however, important to reduce the number of debris to avoid contamination of the IMM, which can affect the quality of the seal of the glass pipette with the membrane. This scanning step under the microscope makes it possible to choose a mitoplast with high IMM integrity recognized by a less dense lobe than the one delimited by the OMM and therefore increases the chances of a successful break-in.

This technique for the first time provided the direct measurement of UCP1- and AAC-dependent H^+ currents within their native membrane. However, mitochondrial integrity and compartmentalization no longer exist due to the rupture of the OMM and probably the cristae. It is therefore essential to complement patch-clamp analysis with other classical methods such as mitochondrial respiration to confirm the physiological role of newly characterized proteins in intact mitochondria.

The patch-clamp technique applied to mitochondria offers new possibilities to better understand the molecular mechanisms responsible for mitochondrial H^+ leak and thermogenesis. Combined with modern cellular and molecular techniques, this innovative approach will provide new insights into the mechanisms that control the thermogenic capacity of mitochondria and how they can be targeted to combat diseases associated with mitochondrial dysfunction.

ACKNOWLEDGMENTS:

I thank Dr. Yuriy Kirichok for the great science I was part of in his lab and the members of the Kirichok lab for the helpful discussions. I also thank Dr. Douglas C. Wallace for providing *AAC1* knockout mice. **Funding**: A.M.B was supported by an American Heart Association Career Development Award 19CDA34630062.

DISCLOSURES:

The author declares no competing interests.

REFERENCES:

1. Divakaruni, A. S., Brand, M. D. The regulation and physiology of mitochondrial proton leak. *Physiology (Bethesda)*. **26** (3), 192–205 (2011).
2. Chouchani, E. T., Kazak, L., Spiegelman, B. M. New advances in adaptive thermogenesis: UCP1 and beyond. *Cell Metabolism*. **29** (1), 27–37 (2019).
3. Cannon, B., Nedergaard, J. Brown adipose tissue: function and physiological significance. *Physiological Reviews*. **84** (1), 277–359 (2004).
4. Nicholls, D. G. The hunt for the molecular mechanism of brown fat thermogenesis. *Biochimie*. **134**, 9–18 (2017).
5. Bertholet, A. M. et al. H(+) transport is an integral function of the mitochondrial ADP/ATP

carrier. *Nature*. **571** (7766), 515–520 (2019).
6. Fedorenko, A., Lishko, P. V., Kirichok, Y. Mechanism of fatty-acid-dependent UCP1 uncoupling in brown fat mitochondria. *Cell*. **151** (2), 400–413 (2012).
7. Bertholet, A. M. et al. Mitochondrial patch clamp of beige adipocytes reveals UCP1-positive and UCP1-negative cells both exhibiting futile creatine cycling. *Cell Metabolism*. **25** (4), 811–822 e814 (2017).
8. Kirichok, Y., Krapivinsky, G., Clapham, D. E. The mitochondrial calcium uniporter is a highly selective ion channel. *Nature*. **427** (6972), 360–364 (2004).
9. Fieni, F., Lee, S. B., Jan, Y. N., Kirichok, Y. Activity of the mitochondrial calcium uniporter varies greatly between tissues. *Nature Communications*. **3**, 1317 (2012).
10. Chaudhuri, D., Sancak, Y., Mootha, V. K., Clapham, D. E. MCU encodes the pore conducting mitochondrial calcium currents. *eLife*. **2**, e00704 (2013).
11. Vais, H., Payne, R., Paudel, U., Li, C., Foskett, J. K. Coupled transmembrane mechanisms control MCU-mediated mitochondrial Ca(2+) uptake. *Proceedings of the National Academy of Sciences of the United States of America*. **117** (35), 21731–21739 (2020).
12. Vais, H. et al. EMRE is a matrix Ca(2+) sensor that governs gatekeeping of the mitochondrial Ca(2+) uniporter. *Cell Reports*. **14** (3), 403–410 (2016).
13. Vais, H. et al. MCUR1, CCDC90A, is a regulator of the mitochondrial calcium uniporter. *Cell Metabolism*. **22** (4), 533–535 (2015).
14. Kamer, K. J. et al. MICU1 imparts the mitochondrial uniporter with the ability to discriminate between Ca(2+) and Mn(2+). *Proceedings of the National Academy of Sciences of the United States of America*. **115** (34), E7960–E7969 (2018).
15. Bertholet, A. M., Kirichok, Y. Patch-clamp analysis of the mitochondrial H(+) leak in brown and beige fat. *Frontiers in Physiology*. **11**, 326 (2020).
16. Mann, A., Thompson, A., Robbins, N., Blomkalns, A. L. Localization, identification, and excision of murine adipose depots. *Journal of Visualized Experiments: JoVE*. (94), 52174 (2014).
17. Garg, V., Kirichok, Y. Y. Patch-clamp analysis of the mitochondrial calcium uniporter. *Methods in Molecular Biology*. **1925**, 75–86 (2019).
18. Decker, G. L., Greenawalt, J. W. Ultrastructural and biochemical studies of mitoplasts and outer membranes derived from French-pressed mitochondria. Advances in mitochondrial subfractionation. *Journal of Ultrastructure Research*. **59** (1), 44–56 (1977).
19. Liu, B. et al. Recording electrical currents across the plasma membrane of mammalian sperm cells. *Journal of Visualized Experiments: JoVE*. (168) (2021).
20. Flaming, D. G., Brown, K. T. Micropipette puller design: form of the heating filament and effects of filament width on tip length and diameter. *Journal of Neuroscience Methods*. **6** (1–2), 91–102, (1982).
21. Klingenberg, M. The ADP and ATP transport in mitochondria and its carrier. *Biochimica and Biophysica Acta*. **1778** (10), 1978–2021 (2008).

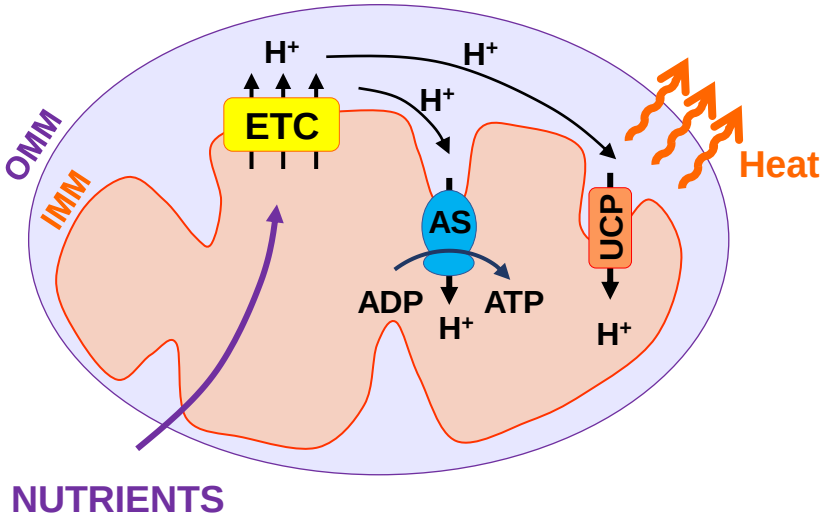

Figure 1.

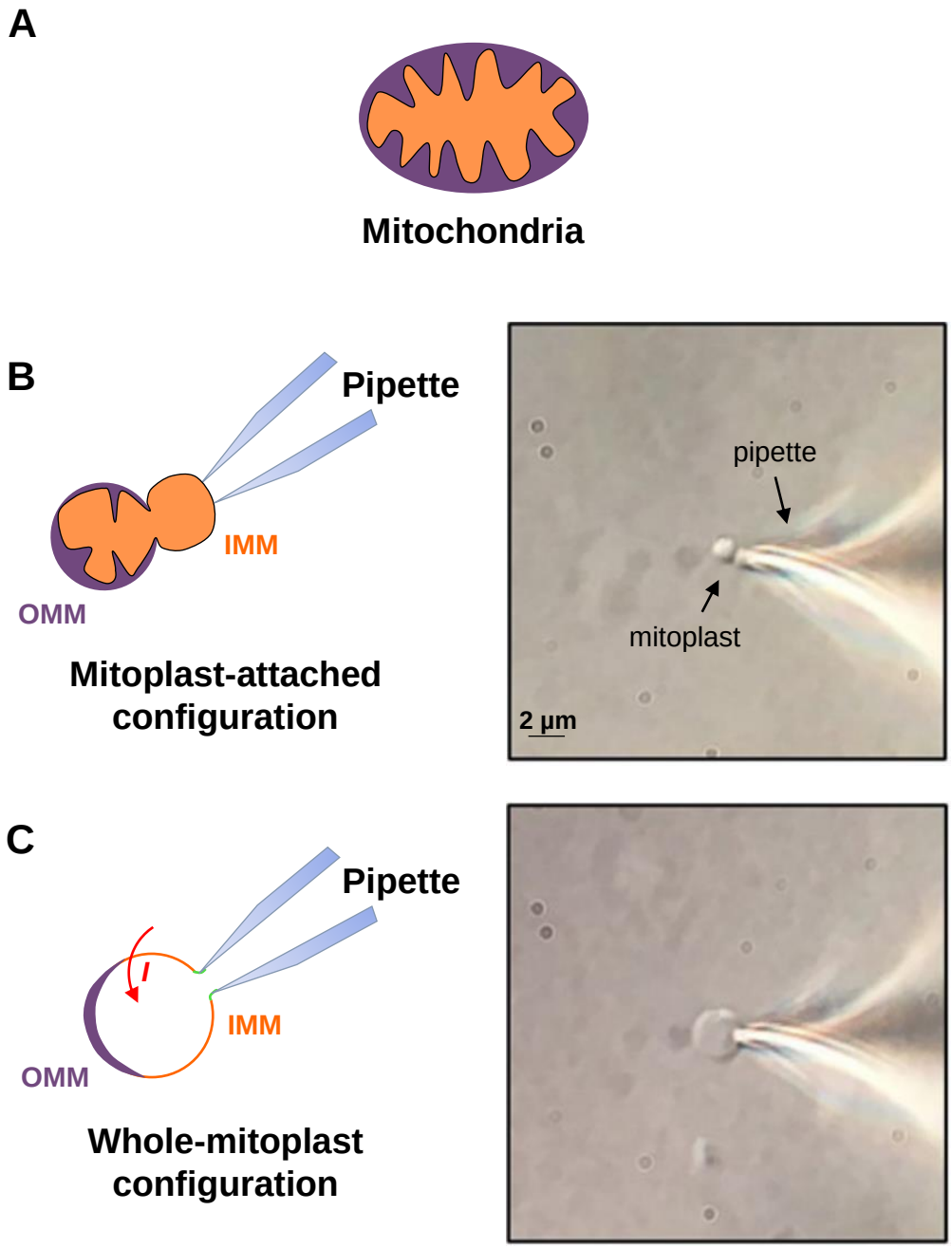

Figure 2.

A

B

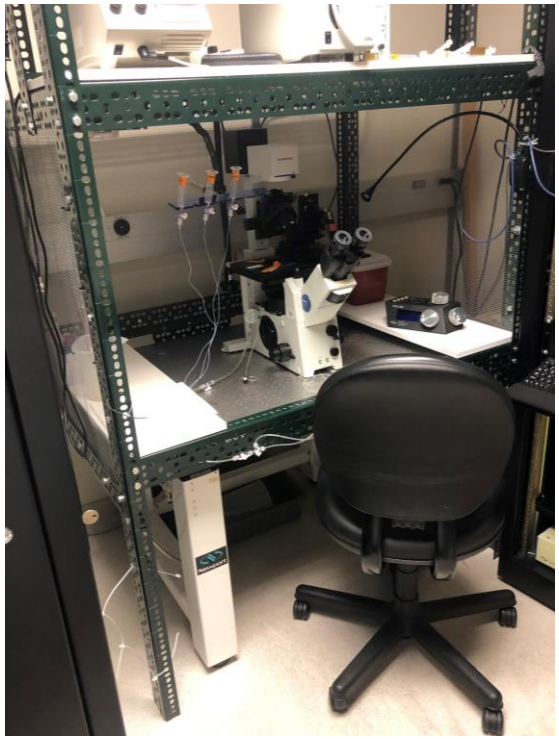

Figure 3.

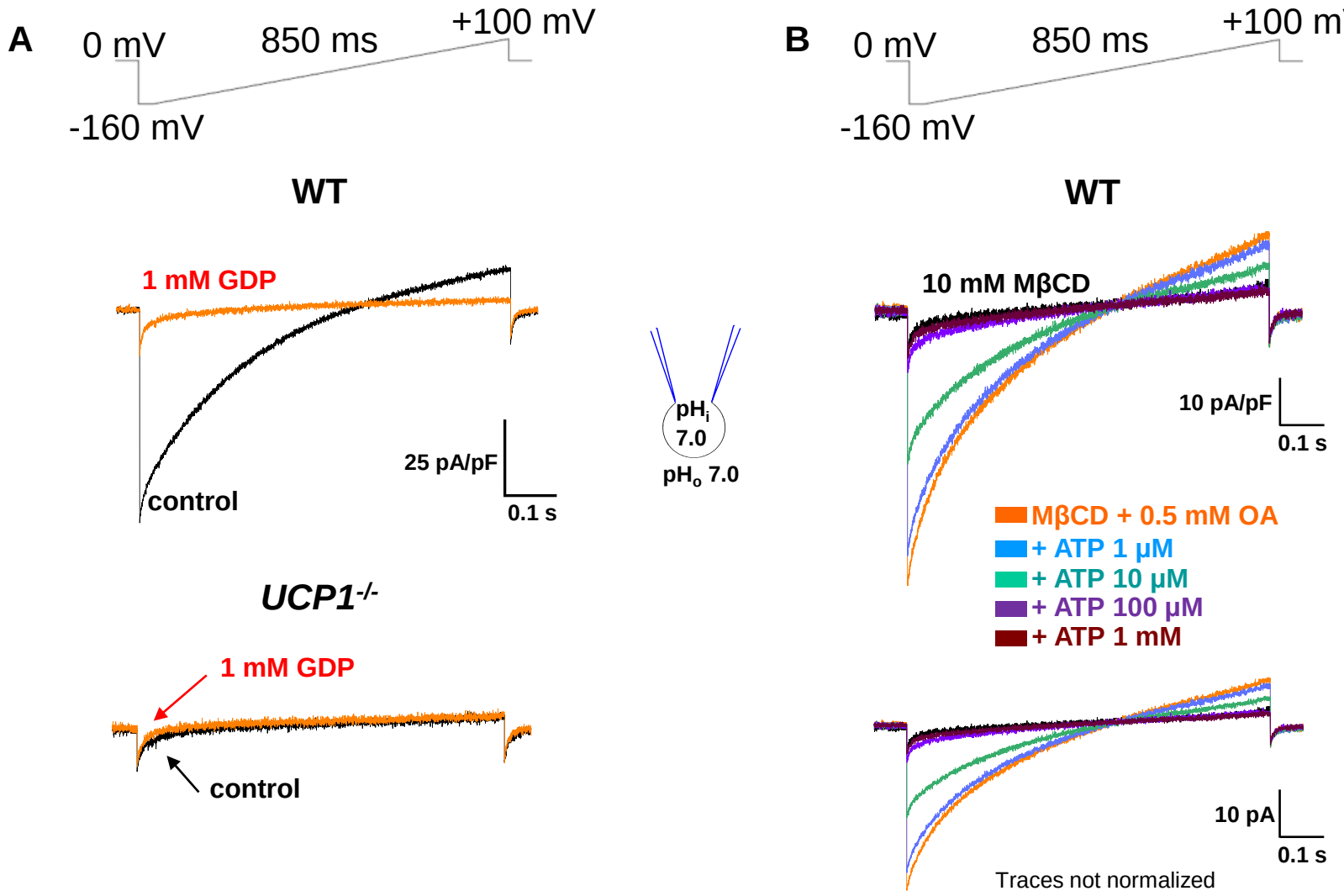

Figure 4.

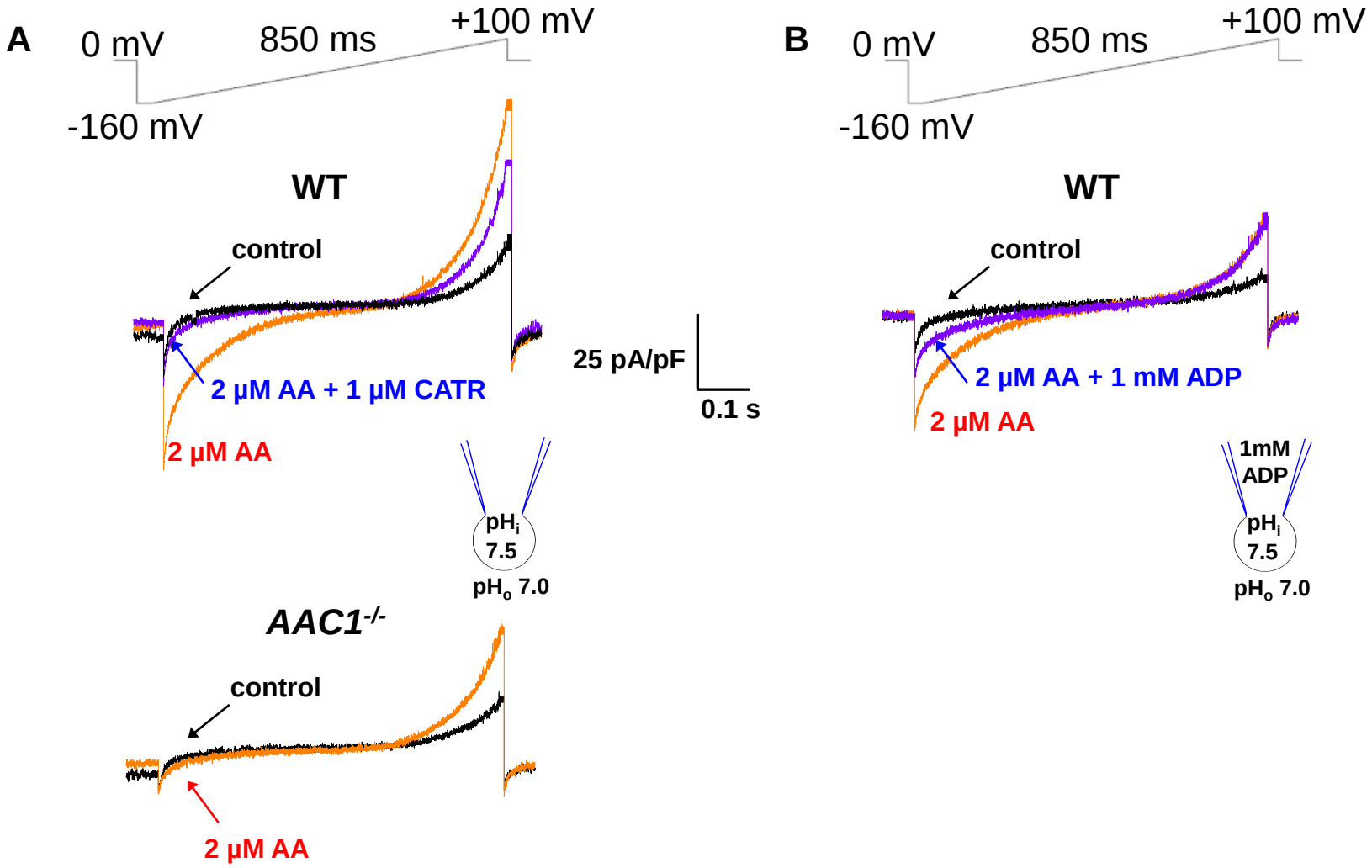

Figure 5.

Reagent	Final concentration
sucrose	250 mM
HEPES	10 mM
EGTA	1 mM
pH adjusted to 7.2 with TrisBase	

Table 1. Mitochondrial isolation buffer (tonicity ~ 300 mmol per kg)

Reagent	Final concentration
sucrose	140 mM
D-mannitol	440 mM
HEPES	10 mM
EGTA	1 mM
pH adjusted to 7.2 with TrisBase	

Table 2. Hypertonic-mannitol buffer

Reagent	Final concentration
KCl	750 mM
HEPES	20 mM
EGTA	1 mM
pH adjusted to 7.2 with TrisBase	

Table 3. Hypertonic-KCl buffer

Reagent	Final concentration
TMA	130 mM
HEPES	100 mM
EGTA	1 mM
$MgCl_2$ for UCP1 recordings or TrisCl for AAC recordings	2 mM
pH adjusted to 7.0 or 7.5 with D-gluconic acid	

Table 4. TMA-based pipette solution (tonicity ~ 360 mmol per kg)

Reagent	Final concentration
KCl	150 mM
HEPES	10 mM
EGTA	1 mM
pH adjusted to 7.0 with TrisBase	

Table 5. KCl bath solution (tonicity ~ 300 mmol per kg)

Reagent	Final concentration
sucrose	100 mM for UCP1 recordings or 150 mM for AAC recordings
HEPES	150 mM for UCP1 recordings or 100 mM for AAC recordings
1 mM EGTA	
pH adjusted to 7.0 with TrisBase	

Table 6. HEPES bath solution (tonicity ~ 300 mmol per kg)

Name of Material/ Equipment	Company	Catalog Number
0.1% gelatin	Millipore	ES-006-B
60X water immersion objective, numerical aperture 1.20	Olympus	UPLSAPO60XW
Axopatch 200B amplifier	Molecular Devices	
Borosilicate glass capillaries	Sutter Instruments	BF150-86-10
Digidata 1550B Digitizer	Molecular Devices	
Faraday cage	Homemade	
French Press	Glen Mills	5500-000011
IKA Eurostar PWR CV S1 laboratory overhead stirrer		
Inversed Microscope	Olympus	IX71 or IX73
Micro Forge	(Narishige)	MF-830
Micromanupulator MPC-385	Sutter Instruments	FG-MPC325
Microelectrode holder for agar bridge	World Precision Instruments	MEH3F4515
Micropipette Puller	(Sutter Instruments)	P97
Mini Cell for French Press	Glen Mills	5500-FA-004
MIXER IKA 6-2000RPM	Cole Parmer	EW-50705-50
Objective 100X magnification	Nikon lens	MPlan 100/0.80 ELWD 210/0
pClamp 10	Molecular Devices	
Perfusion chamber	Warner Instruments	RC-24E
Potter-Elvehjem homogenizer 10 ml	Wheaton	358039
Refrigerated centrifuge SORVALL X4R PRO-MD	Thermo Scientific	75 009 521
Small round glass coverslips: 5 mm diameter, 0.1 mm thickness	Warner Instruments	640700
Vibration isolation table	Newport	VIS3036-SG2-325A

Chemicals	Company	Catalog Number
D-gluconic acid	Sigma Aldrich	G1951

D-mannitol	Sigma Aldrich	M4125
EGTA	Sigma Aldrich	3777
HEPES	Sigma Aldrich	H7523
KCl	Sigma Aldrich	60128
MgCl2	Sigma Aldrich	63068
sucrose	Sigma Aldrich	S7903
TMA	Sigma Aldrich	331635
TrisBase	Sigma Aldrich	T1503
TrisCl	Sigma Aldrich	T3253

Comments/Description

I would like to thank the reviewers for the valuable feedback that will help improve the manuscript. Please find below the point-by-point responses to the comments of the reviewers.

Reviewers' comments:

Reviewer #1:
Manuscript Summary: The author precisely explained methods to measure H+ currents through the mitochondrial inner membrane. Two different examples were demonstrated: one is H+ current through UCP1 in bran fat mitochondria and the other is the one mediated via AD/ATP carrier in heart mitochondria. This is an excellent method paper and very much helpful for mitochondria researchers.

I thank the reviewer for the compliments. The technique described here was optimized by the Kirichok laboratory, which I learned during my postdoctoral training.

Major Concerns: I have no major concerns
Minor Concerns:
1. With the TMA-based pipette solution with 2-4 mM Cl, I am afraid that adjusting zero-current level might be difficult. Did the author use a 3 M KCl-agar salt bridge for the pipette electrode or use conventional Ag/AgCl wire?

This is correct. We use an agar bridge inserted into a microelectrode holder with a 2 mm Ag/AgCl pellet as a reference electrode. The Ag/AgCl pellet molded into the body of the holder provides a more stable low-noise baseline than that obtained with a silver wire. I now indicate in the text the type of pipette holder holding the agar bridge and have referenced the catalogue number in the Excel file of the material.

2. Please explain how the experimental temperature was controlled.

We do not precisely control the temperature of the perfusion chamber with a heating plate. We patch in a room where the temperature is fairly stable and only fluctuates between 22 and 24°C.

3. In my experience, it may be difficult to transfer a thin coverslip (0.1 mm thickness) to the recording chamber. Please explain more how the author performed the transfer.

We use a standard thin microdissection forceps with a curved tip. The coverslip can be broken, especially when learning, but after several tries it is really easy to insert it gently into the bottom of the chamber. I have added a line in the protocol explaining the transfer of the coverslip into the chamber.

Reviewer #2:
Review according manuscript: "Use of the Patch-clamp Technique to Study the Thermogenic Capacity of Mitochondria" by Ambre Bertholet.

Manuscript Number: JoVE62618

In these manuscript, author has been described patch-clamp method with main steps in measuring H+ leak across the inner mitochondrial membrane as a new approach to study the thermogenic capacity of mitochondria.
In seems that patch-clamp methodology applied to mitochondria enabled the opportunity to direct study of proton leak through the inner mitochondrial membrane. It allows describe biophysical and pharmacological properties of mitochondrial transporters like uncoupling protein specific of brown and beige fats. This unique approach will provide new insights into the study of mitochondrial thermogenesis mechanisms
The topic is interesting and important, and the findings have a high impact to broad ranged readers. The experiments are carefully designed and well performed. I believe the scientific merit is worthy for publication in a prestigious journal such as Journal of Visualized Experiments. Generally speaking, the paper is sound; however there are some problems. Main body of the manuscript
Introduction:
In my opinion the introduction lacks a paragraph on the patch-clamp technique, especially in the context of experiments performed on the inner mitochondrial membrane. Such a historical outline would be helpful in enhancing the application of the patch-clamp method in the proposed studies H+ leak across the inner mitochondrial membrane. I suggest adding a paragraph regarding patch-clamp technique and possibilities of its use for potassium or chloride measurements through inner mitochondrial membranes.

Thank you for the constructive comments of the reviewer. As suggested, I have added a paragraph in the introduction about the whole IMM patch-clamp technique established by Yuriy Kirichok in a reproducible way during his postdoctoral training in David Clapham's laboratory. The whole IMM patch-clamp can also be used to measure other conductances across the IMM, such as K^+ and Cl^- currents, but the study of these two conductances with the whole IMM patch-clamp has not yet been published. I have chosen to cite in this review only the bibliography of the whole IMM experiment to support the protocol described here. Several seminal works of the group of Ildiko Szabo, one of the world leaders in K^+ conductances in mitochondria using the electrophysiology approach, are not referenced here, as these studies are mainly based on recordings of single K^+ channels from IMM patches and added channels in lipid bilayers.

Protocol
This part is well prepared. Only, photos are missing here. If possible, I recommend show, for example, a patch-clamp setup, French press and the like. Question: is it possible to use the proposed protocol for H+ transport studies in the inner mitochondrial membrane derived from cell lines? Please extend these issue and add adequate comments to the manuscript, not only in the Discussion section.

I have added a picture of a standard electrophysiological setup used for patch-clamp applied to mitochondria (Faraday cage, microscope, air table) and a picture of a French press.
This protocol can also be applied to cell lines. Historically, the first paper reporting IMM recordings was from COS7 cell lines. I referred in the introductory section when I added a paragraph on the whole IMM patch-clamp. I also mentioned it in the discussion section.

Representative Results
Presented results shows possibilities of measurements of H+ current through inner mitochondrial membrane. How author exclude the possibility of measuring other transporters or channel activities

present in the inner mitochondrial membrane? It is also unclear whether the protons pumped out through the respiratory chain are not a disturbance in the proposed protocol? The above issues requires in-depth discussion in part of the discussion.

Pharmacological studies and the use of KO mice were essential for the characterization and identification of the proteins responsible for the H^+ current through the IMM of various tissues. These studies established that UCP1 is the main UCP of brown and beige fat, and AAC in non-adipose tissues. We cannot completely exclude the possibility of the existence of other H^+ currents not mediated by UCP1 and AAC. However, if other H^+ currents exist, their amplitude was beyond the resolution of our electrophysiological setup. We do not measure H^+ pumping of the ETC under the conditions described in this paper. Once we have reached the full IMM configuration, the mitochondrial matrix is washed out by perfusion of the intra-pipette solution. The intermembrane space no longer exists since the step of breaking the OMM with the French Press. No substrates of the respiratory complexes crucial for H^+ pumping through the ETC have been added. It is therefore unlikely to develop active H^+ pumping under our electrophysiological conditions.
I have added a paragraph to the discussion regarding this issue.

Figures
Red/Green figures are challenging for those with color vision deficiencies. I highly recommend not using the red and green. Here are some helpful items to aid in recoloring: Optimizing color maps with consideration for color vision deficiency to enable accurate interpretation of scientific data (https://journals.plos.org/plosone/article?id=10.1371/journal.pone.0199239) Coloring for colorblindness (https://davidmathlogic.com/colorblind/#%23D81B60-%231E88E5-%23FFC107 %23004D40)

This is modified according to the visible color for persons with color vision deficiencies.

Tables
The fullness of the protocol would be reinforced by the insertion of the catalog numbers of the used proposed chemicals in the tables. It has been prepared brilliantly in table "Name of Material/Equipment". In case "Potter-Elvehjem homogenizer" I suggest add recommended type and volume.

This is done.

Reviewer #3:
This is a proposal to present very important and challenging technique that deals with measuring ionic currents in mitochondrial inner membrane (IMM) with the patch-clamp in whole-mitoplast configuration. This work is extremely important, and author is one of very few researchers world-wide who mastered this approach. Overall methods described in sufficient details and this referee will be looking forward for the video to be published.

Thank you for the reviewer's encouragement.

I have several points that I suggest need to be addressed in the presentation:

1. Pipettes used for mitoplast patch-clamp are much smaller than regular (whole-cell) pipettes. If will be nice if author gave more details regarding the specifics of these pipettes. I hope that video will include images of the pipette tip shape and fire-polishing process. Also, it might be useful if author could give some suggestions regarding strategies on how to adjust the puller settings to achieve proper shape (perhaps initial puller setting and which parameters can be adjusted to achieve desirable shape).

This is done. The video will show pipette tip shape and the fire-polishing process.

2. It does not appear that Axon amplifier is essential. If this is correct may be author could mention that other amplifiers could be used.

The electrophysiological setup we use requires a standard amplifier allowing low noise recordings. Axopatch is used here but Sutter IPA is cited as great by Polina Lishko's recent article in JOVE. I have never experienced it.

3. In the discussion author could reference the original work by Kirichok and Clapham on MCU in which many of the "tricks" to achieve the successful whole-mitoplast configuration were developed for the first time.

I am very grateful to the reviewer for noticing this missing citation. I am very happy to add the pioneering paper by Yuriy Kirichok which, for the first time, shows reproducible recordings of the whole IMM. Being too focused on protons, I forgot to mention this nice article about calcium conductance through the IMM via the MCU.
I added a paragraph telling the story of the mitochondrial patch-clamp as suggested by the reviewer. I have now described and cited Yuriy Kirichok's first paper on mitochondria and other important papers on calcium currents through the IMM in the introduction.

Reviewer #4:
Manuscript Summary: The methods manuscript is excellent. I would recommend a few small changes: Please make one figure at least with a traditional scale bar with current instead of current divided by capacitance. Even though the latter is correct, the former is more familiar to many investigators and would serve as a nice comparison to other published reports.
Can you show a micrograph of the patch electrode on the mitoplast? How is this imaging done during seal formation? Is it performed by looking through the microscope eye pieces or is it performed using a camera and imaging on a monitor (so it can be further enlarged)? Can a micrograph be shown of the field (showing the usual debris and the mitoplast identified amongst the debris)?
This is not important for this manuscript, but I am curious about the difference in the outward current in the heart recordings and why is it not sensitive to carboxyatractyloside?

I thank the reviewer for these great words.
I have added in Figure 4B the same trace not normalized below that represents the UCP1-dependent H^+ current titrated with different ATP concentrations. The brown fat mitoplast in this figure had a membrane capacitance of 0.624 pF.

I have added two photographs in Figure 2 to show what is seen with the microscope equipped with DIC optics. Figure 2B on the left panel shows a schematic of the formation of the gigaohm seal between the glass patch pipette and the IMM (mitoplast-attached configuration). Figure 2B on the right panel shows a photograph of a mitoplast attached to the glass patch-pipette. The pipette is attached to the lobe of the IMM. We use 60X magnification to visualize the IMM lobe which is less optically dense as compared to the lobe that contains both, IMM and the remnants of the OMM. Once the mitoplast of interest is selected, we approach the glass pipette to the mitoplast using a micromanipulator. The whole procedure (the selection of the mitoplast, glass pipette sealing) are performed under the microscope optics. Figure 2C shows the whole-IMM configuration after breaking the IMM with voltage pulses.

The outward current noticed by the reviewer is a very interesting current. The article published in 2019 demonstrated that the outward current CATR-insensitive is not a H^+ current. Both AAC and UCP1 require free fatty acids to induce a H^+ current. Our data suggest that this current is certainly due to FA anion currents at positive voltage (anion inward). We do not know which protein or proteins are responsible for this transport. We have been able to dissociate the outward current (FA anion) from the inward H^+ current by using Mersalyl, a cysteine modifier. We think there is still an outward H^+ current at positive voltages but the amplitude is below pA. Further research will be needed to characterize and identify this FA anion transporter.